CONFIDENTIAL

Copy
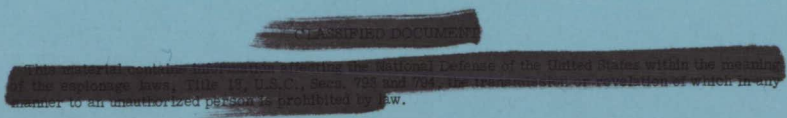RM L58E12a

CASE FILE
COPY

NACA

RESEARCH MEMORANDUM

CASE FILE
COPY

STATIC STABILITY AND CONTROL OF HYPERSONIC GLIDERS

By Robert W. Rainey

Langley Aeronautical Laboratory
Langley Field, Va.

CLASSIFICATION CHANGED TO DECLASSI-
FIED EFFECTIVE JUNE 12, 1963
AUTHORITY NASA CCN-4 BY J. J. CARROL

NATIONAL ADVISORY COMMITTEE
FOR AERONAUTICS

WASHINGTON

July 7, 1958

CONFIDENTIAL

CONFIDENTIAL

NATIONAL ADVISORY COMMITTEE FOR AERONAUTICS

RESEARCH MEMORANDUM

STATIC STABILITY AND CONTROL OF HYPERSONIC GLIDERS*

By Robert W. Rainey

SUMMARY

A study has been made of the static stability and control problems associated with several hypersonic boost gliders. It appears that, in general, it is possible to obtain the desired trim features. The flat-top configuration was found to be essentially self trimming, whereas for the flat-bottom configuration negative camber provided an effective means to trim. Furthermore, at the low angles of attack, directional stability and control were adequate for the complete configurations investigated; however, there is a need for further study of directional stability in the high angle-of-attack range and of lateral stability at all angles of attack.
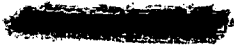
INTRODUCTION

The aerodynamic characteristics of two categories of winged hypersonic boost gliders have been studied. One of these includes moderate range vehicles which operate in the sensible atmosphere at relatively high lift-drag ratios; the other includes vehicles which might be used for manned reentry and do not require high lift-drag ratios. Some aspects of the static stability and control will be presented herein. Considerations of dynamic stability are presented in reference 1.

SYMBOLS

b   wing span

C_D drag coefficient, $\dfrac{\text{Drag}}{q_{\infty}S_W}$

C_L lift coefficient, $\dfrac{\text{Lift}}{q_{\infty}S_W}$

---

*Title, Unclassified.

C_l rolling-moment coefficient, $\dfrac{\text{Rolling moment}}{q_\infty S_W b}$

C_m pitching-moment coefficient, $\dfrac{\text{Pitching moment}}{q_\infty S_W \bar{c}}$

C_n yawing-moment coefficient, $\dfrac{\text{Yawing moment}}{q_\infty S_W b}$

c chord

$\bar{c}$ mean aerodynamic chord

i incidence angle, deg

L/D lift-drag ratio, C_L/C_D

M Mach number

q dynamic pressure

S plan-form area

α angle of attack, deg

β angle of sideslip, deg

δ control deflection angle, deg

Subscripts:

EQ   equivalent

e   elevator

f   flap

N   nose

R   wing root

r   rudder

DECLASSIFIED

w   wing (with tips undrooped for flat-top configuration)

∞   free stream

DISCUSSION

Since a substantial portion of the flight of gliders will be at, or near, trim conditions, it is instructive to consider the approximate range of interest in trim characteristics. (See table I.) In table I, the high-lift-drag-ratio type of glider is envisioned as being the type that operates in the atmosphere at values of trimmed L/D of the order of 5 to obtain ranges of the order of 5,000 nautical miles. The low-lift-drag-ratio type of glider is applicable to global missions or possibly orbital reentry missions. Trimmed angles of attack greater than 45°, as indicated in table I, would undoubtedly be necessary to obtain values of trimmed L/D of the order of one-half for the winged vehicles considered.

High-Lift-Drag-Ratio Type of Gliders

Firstly, a flat-top configuration will be considered (fig. 1). Longitudinal and lateral control is obtained by use of wing-tip flaps. Directional control at subsonic and supersonic speeds is obtained by use of the rudder on the ventral fin. At hypersonic speeds $(M > 6)$, body flaps provide the directional control and may serve as speed brakes at all speeds. Studies of the static stability and control characteristics have been made by Thomas J. Wong of the Ames 10- by 14-Inch Supersonic Wind Tunnel Branch.

The longitudinal stability and control characteristics at trim for this flat-top configuration are presented in figure 2. The open symbols are for results obtained by use of scale models at the Mach numbers indicated. The flagged symbols indicate that the ventral fin was extended. Solid symbols designate results obtained with hypersonically similar models at the equivalent free-stream Mach number as obtained from the hypersonic similarity law. At supersonic speeds, the variation in pitching moment with lift coefficient was reasonably linear and $C_{m_{C_L}}$ was essentially invariant with Mach number. The usual destabilizing shift at subsonic speeds is about 0.05 and the glider is neutrally stable. At subsonic speeds in the high-lift range, however, a pitch-up tendency was found. Elevator deflection required for trim is shown on the lower part of figure 2. The deflections required are small; thus the glider is essentially self-trimming.

Directional stability is shown in figure 3 as a function of equivalent Mach number for two angles of attack, 3° and 7°. It is clear that the glider maintains directional stability throughout the ranges of Mach number and angle of attack shown, although at lower Mach numbers this stability is achieved with the aid of the ventral fin. At Mach numbers around 3, there is some loss in stability with increasing angle of attack.

Lateral stability is shown in figure 4. Here it is observed that C_{l_β} is sometimes positive; that is, the effective dihedral is negative, particularly at the higher Mach numbers and lower angles of attack. Some roll instability is, therefore, indicated. Automatic roll stabilization for the glider has been studied, but the situation is complicated by the fact that the roll controls are located on the drooped wing tips. Thus, aileron deflection produces yawing as well as rolling moments. A satisfactory roll-stabilization scheme was found only after both the ailerons and body-flap controls were employed in combination.

Secondly, a flat-bottom configuration is considered (fig. 5) which has negative camber to provide trim, trailing-edge flaps for longitudinal and lateral control, and rudders on the toed-in wing-tip fins for directional control.

Calculations of the longitudinal stability characteristics of the basic body-wing combination without negative camber have been made at free-stream Mach numbers from 6.9 to 18. The configuration is shown in figure 6 along with the flow fields assumed in the theoretical analysis. It was assumed that the half-cone and cylinder of the body operated in the local flow of the upper wing surface throughout the ranges of α and M. The interference region is shown shaded and bounded by the inviscid shock wave generated by the nose cone and the average expansion from the cone-cylinder juncture. Constant pressure was assumed in the region between the two average expansions as well as between the wing leading edge and nose-cone shock waves. Two-dimensional analysis was applied to the lower wing surface. Finally, through the use of experimental results, the induced effects and effects of leading-edge shock detachment were included. This was accomplished by first plotting the ratio of measured C_L to calculated C_L (using two-dimensional shock-expansion theory) as a function of the hypersonic similarity parameter M_α (where $M_\alpha = M$ times α in radians) for the wings of reference 2. This ratio of measured C_L to calculated C_L was plotted for each wing, and each curve was designated as having a specific value of M_ϵ (where $M_\epsilon = M$ times ϵ in radians, and ϵ is the wing half-apex angle). Then, by use of the hypersonic similarity relations, M_α and M_ϵ, the appropriate C_L ratios were obtained and multiplied times the calculated values for

C_L of the vehicle at the four Mach numbers and various angles of attack. Application of this C_L ratio was also made to the pitching moments.

In figure 7 it is indicated that the calculations predicted C_m very well and overestimated C_L somewhat. The Mach number effects upon C_m are small and C_L is reduced somewhat as the Mach number is increased. It is also noted that in the desired range of trim C_L (around 0.08), there is a sizeable pitching moment to be trimmed out.

The use of several devices considered for trim and control are shown in figure 8. The trailing-edge flaps may be considered for longitudinal and lateral control; in this instance some means must be provided for directional stability and control. The three wing-tip-mounted controls may be considered for longitudinal, lateral, and directional stability and control.

In figures 9 and 10 are presented the characteristics of the configuration with these controls at deflection angles of 0° and -20° at $M_\infty = 6.9$. These results demonstrate the inability of these controls to produce trim in the desired lift-coefficient range of about 0.08. The highest values of trim C_L were obtained with the trailing-edge flap, and this was only about 0.045.

Obviously a better method for trim is required, and the use of negative camber appears adequate as shown in figure 11. The measured and calculated results of the same configuration untrimmed and trimmed by the use of negative camber are presented. By this means a trim lift coefficient of about 0.09 and a trim angle of attack of about 9° were obtained and may be accurately predicted. A loss in stability was realized by trimming; however, the configuration is longitudinally stable at trim. Similar results were obtained at $M_\infty = 9.6$.

In figure 12 are presented the measured and predicted C_{n_β} characteristics of the configuration without and with two types of tip controls. For these predictions, the assumptions for the flow field were similar to those for the longitudinal calculations. It is seen that the configuration without controls is directionally unstable. The directional stability parameter C_{n_β} with either control is about the same at $M_\infty = 6.9$ and essentially invariant with Mach number. The predictions of C_{n_β} are conservative. Additional results at $M_\infty = 6.9$ indicated that the use of negative camber had little effect upon C_{n_β}. Also, the control effectiveness parameter $C_{n_{\delta_r}}$ appeared to be adequate and was predicted with reasonable accuracy by using conical-flow theory for the tip cones and oblique-shock relations for the tip fins at $M_\infty = 6.9$. Some additional results of

wind-tunnel tests at $M_\infty = 6.9$ indicate that C_{n_β} increases with α in the α range from $0°$ to $16°$ and that the configuration had positive dihedral effect at α greater than $5°$.

Low-Lift-Drag-Ratio Type of Gliders

Consider now the low-lift-drag-ratio type of vehicles which may operate in the atmosphere or might also be considered as orbital reentry vehicles. As indicated in table I, it appears desirable for these vehicles to trim at angles of attack from $20°$ to $45°$, or greater, at lift coefficients of from about 0.3 to 0.8.

In figure 13 are presented two configurations which are of the low-lift-drag-ratio type. For the vehicle on the left, trim is accomplished by the use of trailing-edge flaps; the combined use of deflected nose and flaps accomplishes trim for the vehicle on the right. In both instances, the flaps in the upper and lower surfaces deflect in the same direction. Cavities (shown as darkened regions on the rear of the vehicles) provide a means to deflect the flaps within the vehicles. Both vehicles were directionally stable at $\alpha = 0°$ (no results for $\alpha > 0°$). Directional control was accomplished by deflecting the rearward portion of the leading edges (shown by dashed lines in the plan views in fig. 13).

The experimental results in figure 14 indicate for this vehicle a trim capability at C_L of about 0.2 at an angle of attack of about $15°$ with the flaps deflected $-20°$. For the other vehicle (fig. 15), a trim C_L of about 0.45 and a trim α of about $30°$ was obtained with $i_N = 20°$ and $\delta_f = -10°$. Extrapolation of additional measured results (with $i_N = 20°$ and $\delta_f = -20°$) show a trim capability at a C_L greater than 0.7 and an α in excess of $45°$. For both vehicles, optimization of the combination of nose and flaps would undoubtedly increase the attainable trim C_L and α.

CONCLUDING REMARKS

It appears that, in general, it is possible to obtain the desired trim features. The flat-top configuration was found to be self-trimming, whereas for the flat-bottom configuration negative camber provided an effective means to trim. Furthermore, at the low angles of attack, directional stability and control are adequate for the complete configurations investigated; however, there is a need for further study of

directional stability in the high angle-of-attack range and of lateral stability at all angles of attack.

Langley Aeronautical Laboratory,
National Advisory Committee for Aeronautics,
Langley Field, Va., March 18, 1958.

REFERENCES

1. Moul, Martin T., and Paulson, John W.: Dynamic Lateral Behavior of High-Performance Aircraft. NACA RM L58E16, 1958.

2. Bertram, Mitchel H., and McCauley, William D.: An Investigation of the Aerodynamic Characteristics of Thin Delta Wings With a Symmetrical Double-Wedge Section at a Mach Number of 6.9. NACA RM L55B14, 1955.

TABLE I

DESIRED CHARACTERISTICS AT TRIM

PARAMETER	TYPE OF BOOST GLIDER	
	HIGH $\frac{L}{D}$	LOW $\frac{L}{D}$
$\frac{L}{D}$	4 TO 6	.5 TO 2
α, DEG	6 TO 9	20 TO 45
c_L	0.06 TO 0.09	$\approx$ 0.3 TO 0.8

FLAT-TOP GLIDER
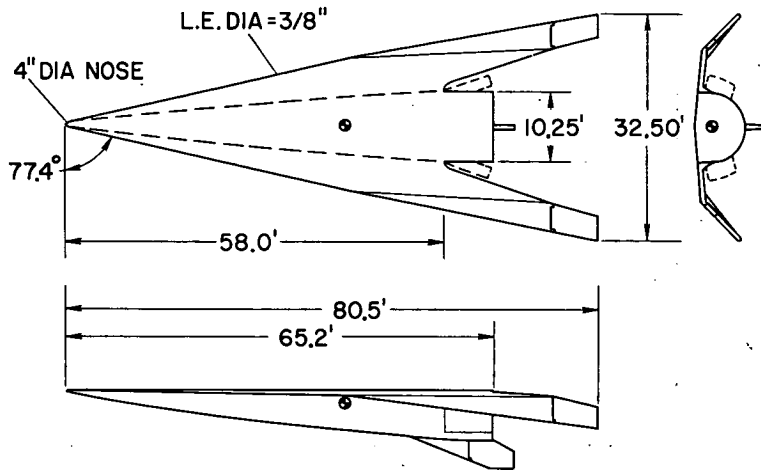
Figure 1

LONGITUDINAL STABILITY AND CONTROL

C G AT 0.76 c_R

Figure 2

DIRECTIONAL STABILITY

Figure 3

LATERAL STABILITY

Figure 4

DECLASSIFIED
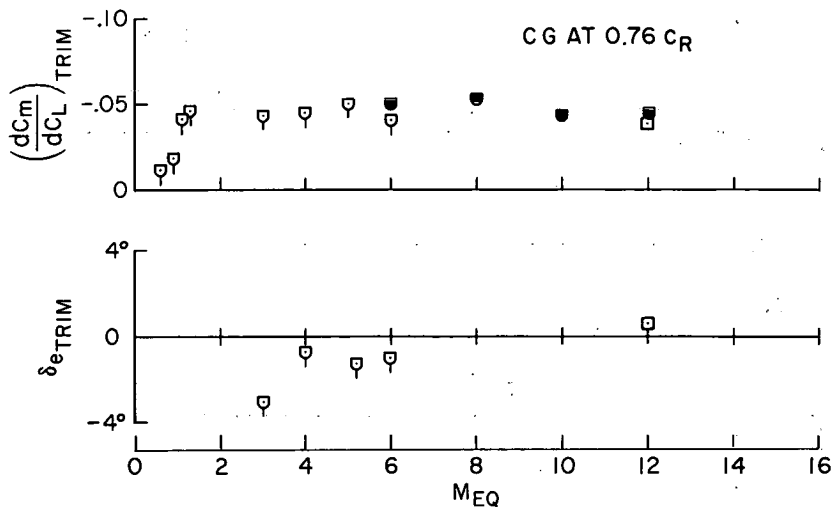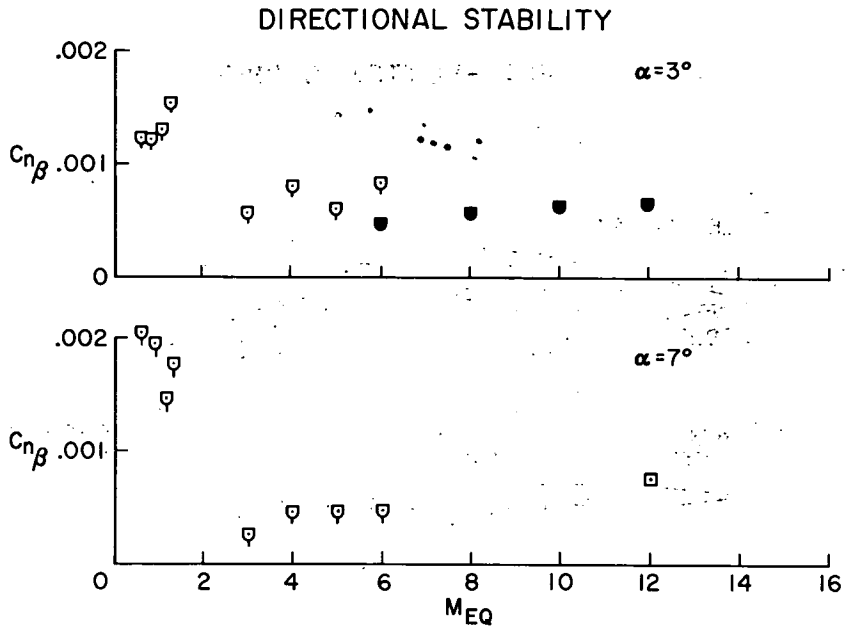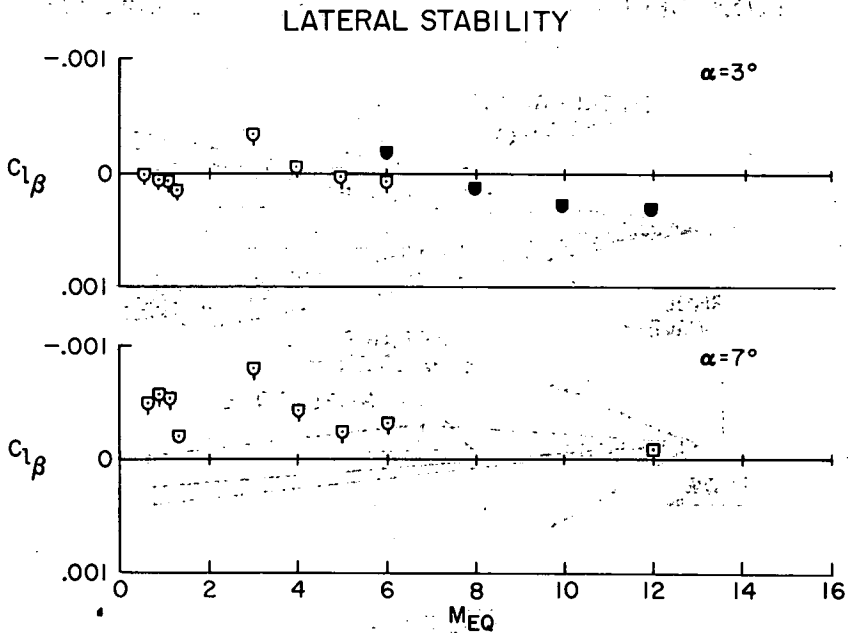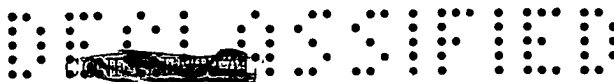
FLAT-BOTTOM GLIDER
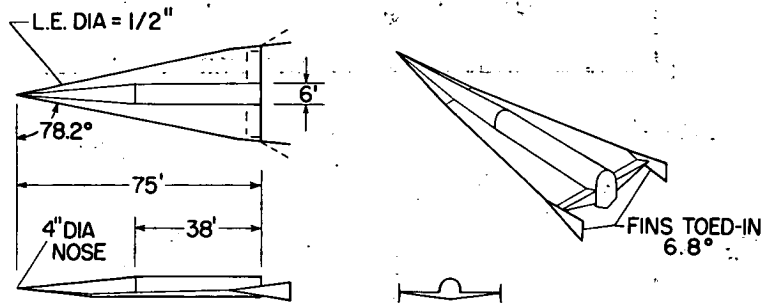
Figure 5

FLOW FIELDS ASSUMED IN THEORETICAL ANALYSIS
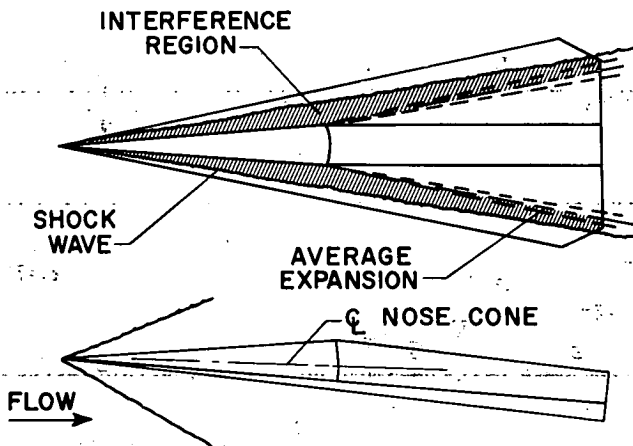
Figure 6

COMPARISON OF CALCULATED AND MEASURED
LONGITUDINAL AERODYNAMIC CHARACTERISTICS
c.g. AT 0.42 $\bar{c}$
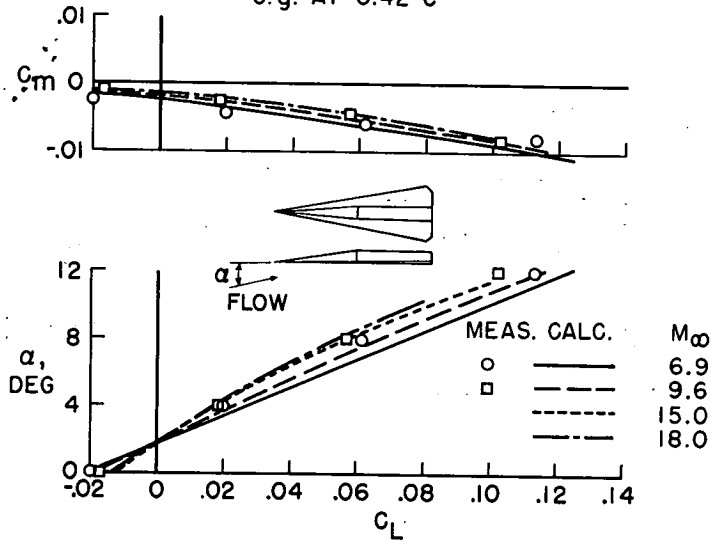
Figure 7

STABILIZING AND CONTROL DEVICES

BODY-WING
(T.E. FLAPS)

BODY-WING-CONE

BODY-WING-TRIPANEL

BODY-WING-PYRAMID
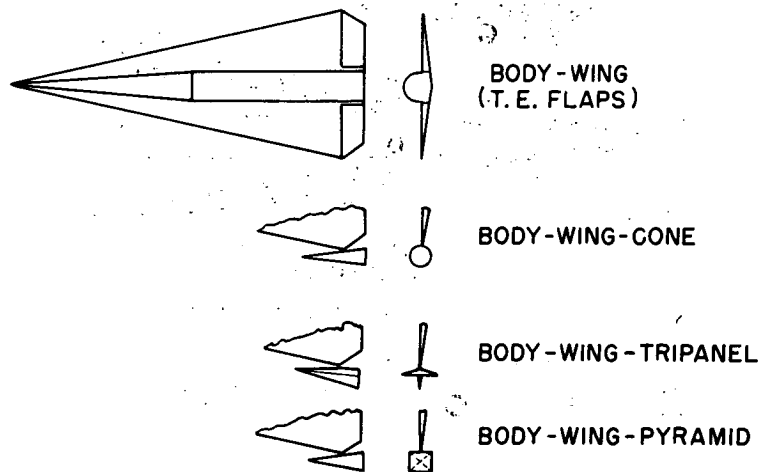
Figure 8

EFFECT OF CONTROL ON LONGITUDINAL
AERODYNAMIC CHARACTERISTICS
$M_\infty = 6.9$; C.g. AT $0.42 \bar{c}$
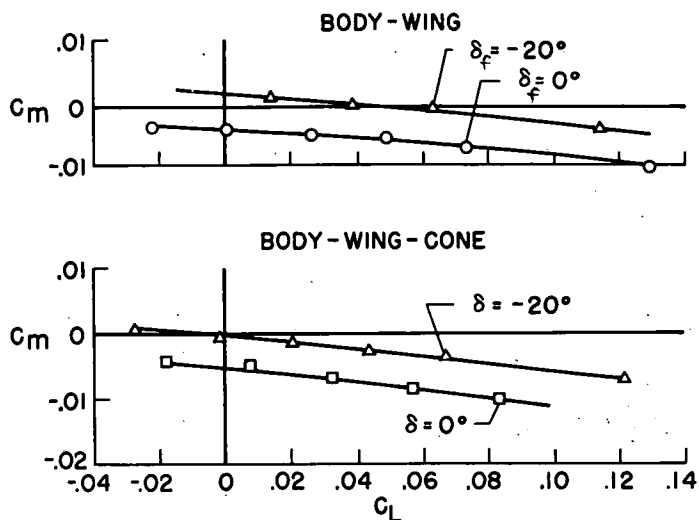
Figure 9

EFFECT OF CONTROL ON LONGITUDINAL
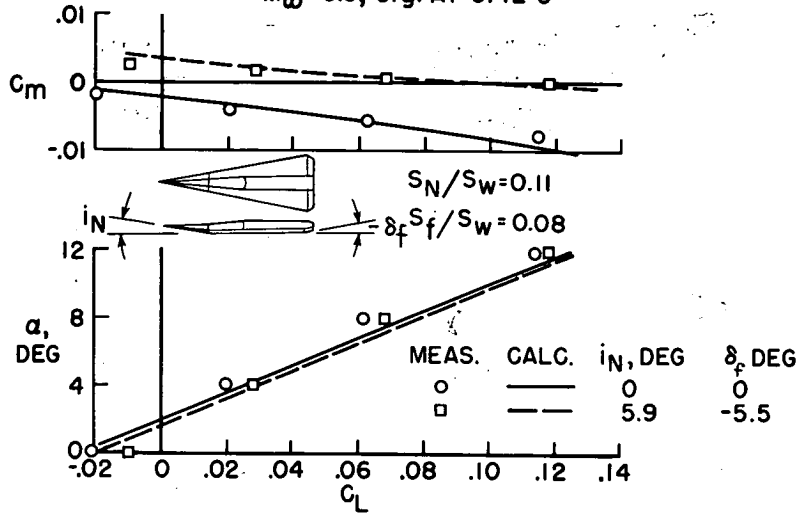AERODYNAMIC CHARACTERISTICS
$M_\infty = 6.9$; C.g. AT $0.42 \bar{c}$
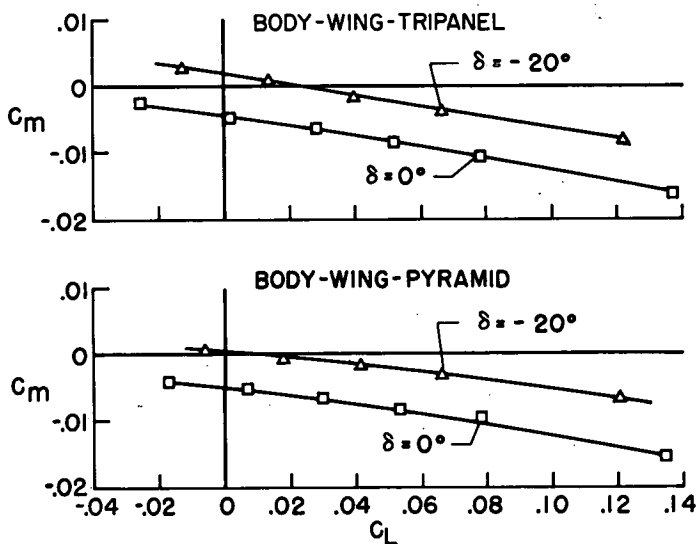
Figure 10

EFFECT OF NOSE AND FLAP INCIDENCES UPON
LONGITUDINAL AERODYNAMIC CHARACTERISTICS

$M_\infty = 6.9$; c.g. AT 0.42 $\bar{c}$

$S_N/S_W = 0.11$

δ_f $S_f/S_W = 0.08$

MEAS.	CALC.	i_N, DEG	δ_f DEG
○	——	0	0
□	— —	5.9	-5.5

Figure 11

EFFECT OF TIP CONTROLS ON
DIRECTIONAL STABILITY AT $\alpha = 0°$
c.g. AT 0.42 $\bar{c}$
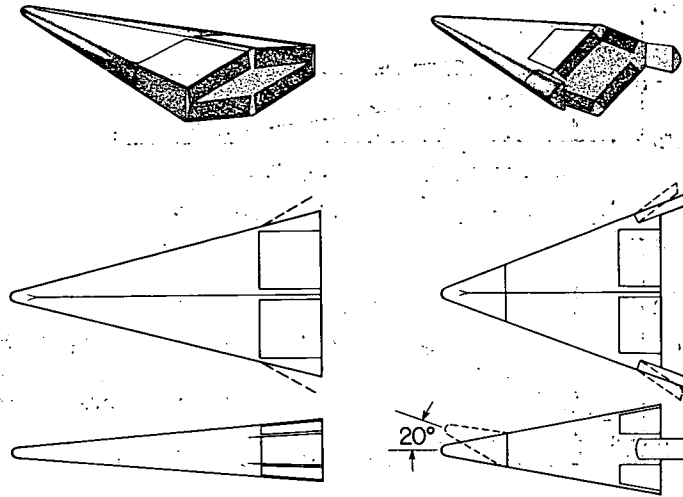
FINS TOED-IN
6.8°
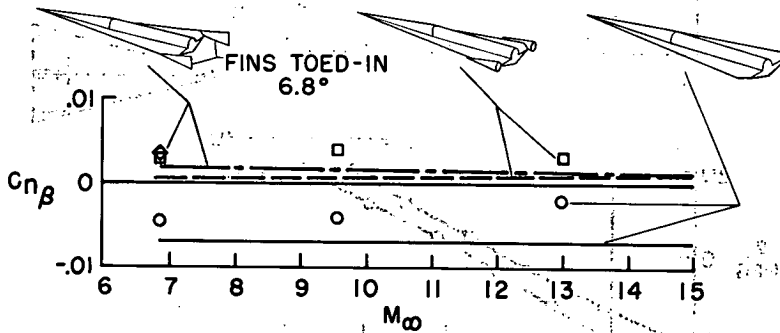
Figure 12

HYPERSONIC BOOST GLIDER

Figure 13

LONGITUDINAL AERODYNAMIC CHARACTERISTICS
OF BOOST-GLIDER WITH LOW LIFT-DRAG RATIO
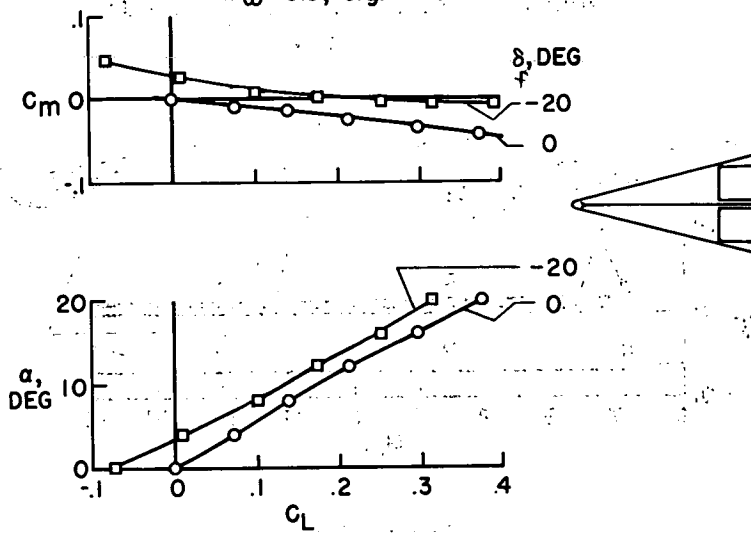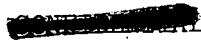$M_\infty = 6.9$; c.g. AT $0.40\bar{c}$

Figure 14
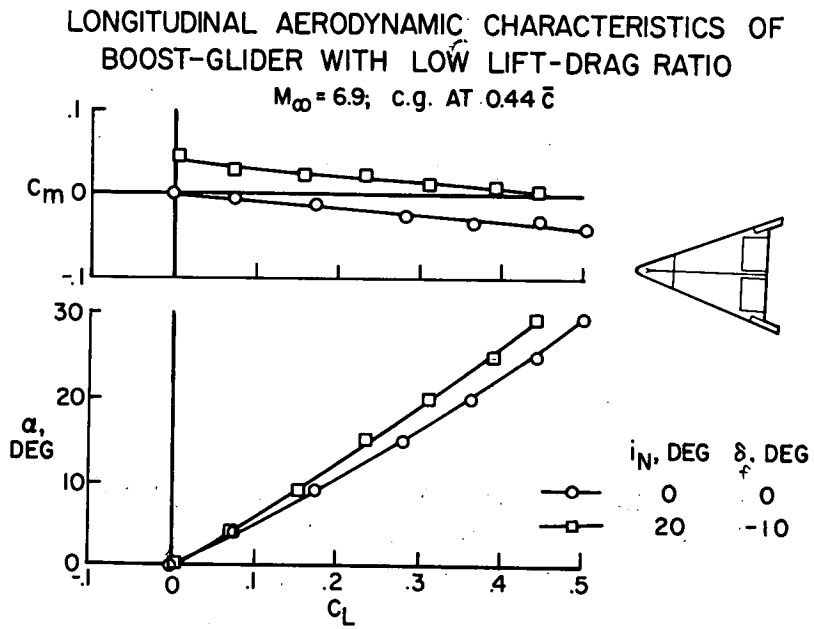
LONGITUDINAL AERODYNAMIC CHARACTERISTICS OF
BOOST-GLIDER WITH LOW LIFT-DRAG RATIO

Figure 15